

Modelling and analysis of solar cells based on GaAs/p-Si: impact on arc dependency

F. M. Rahimi ^a, M. Z. M. Yusoff ^{a,b,c,*}, M. S. Yahya ^s, M. M. I. Sapeli ^e,
N. Zulkepli ^e

^a*School of Physics and Material Studies, Faculty of Applied Sciences, Universiti Teknologi MARA, 40450 Shah Alam, Malaysia*

^b*Institute for Biodiversity and Sustainable Development (IBSD), Universiti Teknologi MARA, 40450 Shah Alam, Malaysia*

^c*Institute of Science (IOS), Universiti Teknologi MARA, 40450 Shah Alam, Malaysia*

^d*Energy Storage Research Group, Faculty of Ocean Engineering Technology and Informatics, Universiti Malaysia Terengganu, 21030, Terengganu, Malaysia*

^e*Centre of Foundation Studies, Universiti Teknologi MARA Cawangan Selangor, Kampus Dengkil, 43800, Dengkil, Selangor, Malaysia*

In this work, various anti-reflection coatings, a single-layer anti-reflective coating (SLARC), and a double-layer anti-reflective coating (DLARC) were used to optimise the efficiency performance of GaAs/p-Si based solar cells using the PC1D simulator. PC1D simulation software is used to simulate the GaAs/p-Si solar cell structures. The different types of ARCs were applied to GaAs/Si solar cells using the ZnO SLARC and ZnO/TiO₂ DLARC. The highest efficiency recorded is 23.42%, achieved by the ZnO SLARC with a thickness of 78.411 nm at a wavelength of 600 nm. This is closely followed by the ZnO/TiO₂ DLARC, which exhibits a slightly lower efficiency of 23.04% at a wavelength of 500 nm, with thicknesses of 63.516 nm and 50.403 nm, respectively. The I-V curves showed that ZnO SLARC and ZnO/TiO₂ DLARC had higher current responses compared to without ARC. We found that both ARC schemes have the potential to reduce the reflection loss and increase the performance of GaAs/Si-based solar cells.

(Received March 27, 2025; Accepted May 16, 2025)

Keywords: Gallium arsenide, GaAs, Silicon, PC1D, Wafer ray tracer, Solar cells

1. Introduction

The use of anti-reflection coatings (ARCs) in solar cell fabrication is one of the popular methods to enhance the production of energy [1]. ARC using nanomaterials has proven to reduce the reflection and enhance the output power produced by Si solar cells [2]. The ARC is one way to reduce reflection losses resulting from reflection on the top layer of silicon. Without ARC, silicon can only transfer roughly 70% of infrared (IR) and 50% of ultraviolet (UV) radiation into the solar cell [3]. Thus, ARC plays a vital role in enhancing the efficiency of solar energy cells by reducing reflection losses [3]. Gallium arsenide (GaAs) is a semiconductor that has a bandgap of 1.42 eV, making it particularly suitable for applications in solar cells. GaAs-based solar cells are frequently chosen over silicon-based alternatives due to a number of advantages. These include a straight bandgap, which improves its efficiency in converting sunlight to electricity, and enhanced carrier mobility when compared to silicon, leading to improved performance. Furthermore, GaAs can work successfully across a larger temperature range and has a better absorption efficiency than silicon, making it ideal for high-performance solar energy systems [4]. GaAs, with a direct bandgap of 1.42 eV, has greater electron mobility and absorption efficiency, making it ideal for the n-region, where effective light absorption and electron transport are critical. Conversely, silicon, defined by its mature technology, affordability, and commendable bandgap of 1.1 eV, offers a reliable and effective basis for the p-region [5].

* Corresponding author: mzmy83@gmail.com
<https://doi.org/10.15251/JOBM.2025.172.77>

The integration of GaAs and Si facilitates the creation of a high-performance solar cell that leverages the optimal characteristics of both materials, leading to enhanced overall efficiency and stability [6]. Anti-reflective coatings (ARCs) improve solar cell performance by reducing reflection losses and increasing light absorption. These thin films are intended to decrease the quantity of light reflected from the solar cell's surface, allowing more light to enter the cell and be converted into energy. ARCs are extensively employed in semiconductor technology to mitigate issues related to light reflection. Researchers anticipate that integrating ARCs with solar cells will enhance their overall performance and energy conversion efficiency. Numerous more coating models exist beyond the singular ARC model. One of these is the dual-layer ARC model. The coating, together with the surface inclination angle and the solar panel, significantly influences the efficiency of the solar cell. Sharma et al. investigated the DLARC of Si_3N_4 at many angles, where the angle of incidence corresponded to the angle of reflection. The conversion efficiency diminished by 1.7% as the angle increased from 0° to 60° [1]. Maiga et al. examined the DLARC and angle, concluding that they are superior to single-layer alternatives [7]. Prior research often utilised identical materials in both the p-type and n-type regions. The preliminary modelling findings of Ibraheem (2020) suggest that solar cell efficiency is approximately 15.39%. TiO_2 SLARC with a back surface field has improved the efficiency of low-cost Si solar cells [16]. In this study, we employ silicon for the p-region and GaAs n-regions to investigate the combined impact on solar cell performance. Various ARCs, including SLARC, DLARC, and even triple-layer ARCs, are used in research to assess their efficiency in improving the efficiency of solar cells [8]. Silicon dioxide (SiO_2), magnesium fluoride (MgF_2), titanium dioxide (TiO_2), zinc oxide (ZnO), and other materials are routinely used for ARCs, each with their set of qualities that can affect solar cell efficiency. Materials used for bilayer ARC consist of $\text{MgF}_2/\text{SiO}_2$, $\text{Al}_2\text{O}_3/\text{TiO}_2$, and MgF_2/ZnS , while $\text{MgF}_2/\text{Al}_2\text{O}_3/\text{ZnS}$ and $\text{GaInP}/\text{GaAs}/\text{Ge}$ are examples of triple ARC materials [9]. Figure 1 illustrates the propagation of light within a monolayer thin film. There are three forms of light direction: light transmission from air to material, light traversing through the ARC, and light penetrating the substrate. Light reflection occurred at the interface between the ARC and the substrate. The refractive indices of the ARC and substrate differ. The refractive index between air and ARC differs as well. This disparity may lead to a modification in the trajectory of refracted and reflected light.

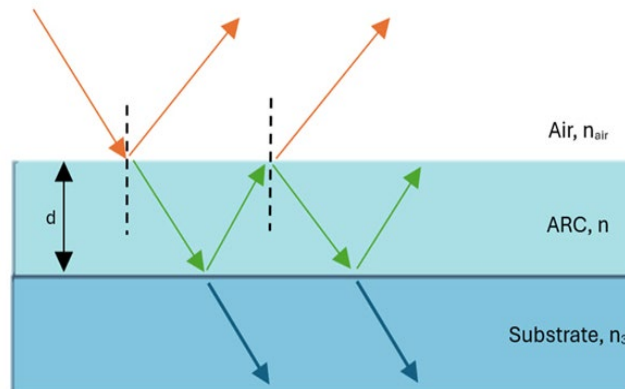


Fig. 1. The illustration of the diffusion of light in a single-layer thin film.

2. Experimental details

Figure 2 illustrates the GaAs/p-Si solar cell used in this work. In this work, the base layer of the solar cell was made of p-Si while the emitter layer was made of n-GaAs. The area for the solar cell device has been set in Table 1, which is 10 cm^2 . The bandgap of the GaAs and Si, which are 1.424 eV and 1.124 eV, respectively, have been used in this simulation. The Si substrate thickness is $150 \text{ }\mu\text{m}$, and for the GaAs substrate, it is $0.1 \text{ }\mu\text{m}$. For the doping concentration, n-region and p-region have been set to $1 \times 10^{16} \text{ cm}^{-3}$ for n-regions and $1 \times 10^{17} \text{ cm}^{-3}$ for p-regions. Table 1 shows the

material inputs used to simulate heterostructure device. The roles of n-GaAs and p-Si layers are to make a pn-junction, which is the main element to generate current when exposed to sunlight. Meanwhile, the ARC layer is used to reduce the reflection and capture more incident light in order to produce more current. To develop the ARC layer, the following equations were used to compute its thickness and refractive index [10]. Refractive index of ARC.

$$\eta_{ARC} = \sqrt{(\eta_{air} * \eta_{Si}(\lambda_0))} \quad (1)$$

Thickness of ARC

$$d = \lambda_0 / 4 * \eta_{ARC} \quad (2)$$

where η_{ARC} and η_{air} are the refractive index of ARC [11]. Further examination of Eq. (1) reveals that the refractive index of ARC is impacted by both the refractive index of air and the wavelength-dependent refractive index of the particular anti-reflection coating [11]. PC1D is a handy software for simulating solar cells developed by the University of New South Wales in Sydney, Australia. It models photovoltaic devices in one dimension and offers libraries of parameters for materials such as GaAs, a-Si, AlGaAs, Si, InP, and Ge. The package also contains solar spectrum files like AM0 and AM1.5. Simulations are conducted using AM1.5 solar radiation with a light intensity of 0.1 W/cm² at room temperature. PC1D version 5 makes comparing simulated and experimental Internal Quantum Efficiency (IQE) curves easier by displaying them on a single graph. To match the experimental data, the model requires higher rear optical reflectance and lower front-surface recombination velocity at shorter wavelengths [13]. A solar cell's maximum power (P_{max}), open circuit voltage (V_{oc}), and short circuit current (I_{sc}) are all measures of how well it performs. The fill factor and efficiency are computed in the study using a certain equation. The equation gives the fill factor's equation [4]. The solar cell's efficiency may then be estimated using the fill factor (3) [13].

$$FF = P_{mp} / I_{sc}V_{oc} = I_{sc}V_{oc} FF / P_{in} \quad (4)$$

$$P_{max} = \text{percentage } \eta \times P_{in} \quad (5)$$

$$P_{in} = \text{Standard Insolation} \times \text{Area of Panel} \quad (6)$$

$$\text{Standard Insolation} = 1\text{kW/m}^2 \quad (7)$$

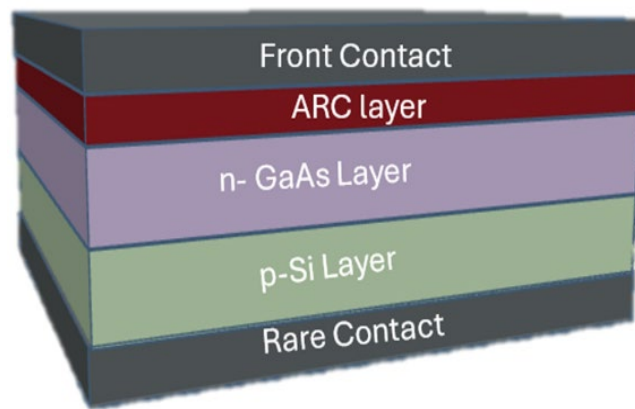


Fig. 2. A diagram of a GaAs/p-Si-based solar cell.

3. Results and discussion

The data output of open circuit voltage (V_{oc}), maximum power output (P_{max}), short circuit current (I_{sc}), and efficiency (η) of no ARC was presented in Table 2. In Table 2, the results of simulating a solar cell without an anti-reflective layer using PC1D software are shown. The results for V_{oc} , P_{max} , and I_{sc} were 0.7476V, 0.1643W, and 0.2527A, respectively. The efficiency, which is 16.43%, is also the lowest efficiency. A solar cell with no anti-reflective coating (ARC) often has a lower efficiency than one with an ARC [14]. This is because without an ARC, a considerable part of incident light is reflected back, resulting in less light absorption and, as a result, lower efficiency when converting light into energy [9]. Figure 3 shows the electrical characteristic of GaAs/Si solar cells without ARC layer. According to Table 3, the result shows ZnO SLARC has the highest efficiency, which is 23.42%. The wavelength (λ) that gets the highest efficiency is at 600 nm, and the results for V_{oc} and I_{sc} were 0.7553 V and 0.3618 A, respectively. Next, the second highest efficiency, which is 23.27% at the wavelength of 700 nm, and the V_{oc} and I_{sc} were 0.7551 V and 0.3593 A, respectively.

Table 2. Result data output of no ARC.

I_{sc} (A)	V_{oc} (V)	P_{max} (W)	Efficiency (%)
0.2575	0.7476	0.1643	16.43

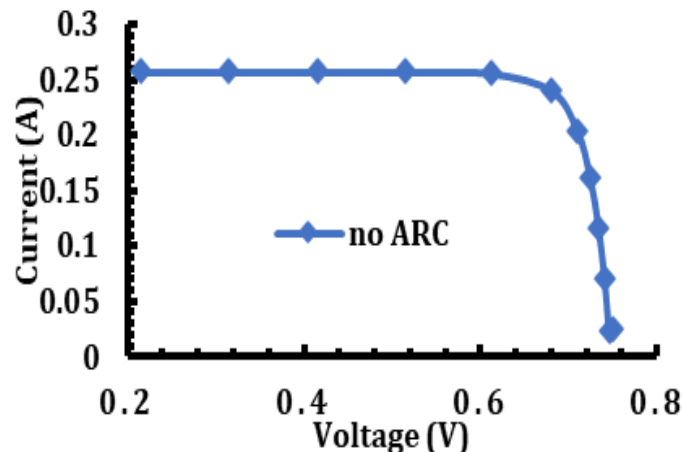


Fig. 3. I-V characteristic for GaAs/Si solar cells without ARC.

Table 3. Result data output of SLARC ZnO.

λ (nm)	Refractive Index	Thickness (nm)	I_{sc} (A)	V_{oc} (V)	Efficiency (%)
250	2.388	26.173	0.2795	0.7495	17.93
300	2.404	31.198	0.2908	0.7504	18.73
400	2.114	47.304	0.3132	0.752	20.12
500	1.968	63.516	0.3515	0.7546	22.79
600	1.913	78.411	0.3618	0.7553	23.42
700	1.883	92.937	0.3593	0.7551	23.27
800	1.864	107.296	0.3488	0.7545	22.63
900	1.851	121.556	0.335	0.7536	21.69

Results of double-layer ARC (DLARC) ZnO/TiO are shown in Table 4. The highest efficiency is at the 500 nm wavelength, which is 23.04%, followed by the 600 nm wavelength, which is 22.74% efficiency. Result for V_{oc} and I_{sc} at 500 nm was 0.7549 V and 0.3555 A, respectively.

Table 4. Result data output of ZnO/TiO, DLARC.

λ (nm)	ZnO		TiO ₂		I _{sc} (A)	V _{oc} (V)	Efficiency (%)
	Refractive Index	Thickness (nm)	Refractive Index	Thickness (nm)			
250	2.388	26.173	2.46	25.407	0.3374	0.7537	21.85
300	2.404	31.198	3.326	22.55	0.03151	0.7522	20.24
400	2.114	47.304	2.68	37.213	0.3548	0.7548	23.00
500	1.968	63.516	2.48	50.403	0.3555	0.7549	23.04
600	1.913	78.411	2.404	62.396	0.3506	0.7546	22.74
700	1.883	92.937	2.364	74.027	0.3447	0.7542	22.36
800	1.864	107.296	2.341	85.434	0.3379	0.7537	21.89
900	1.851	121.556	2.325	96.774	0.3336	0.7535	21.59

Figure 4 indicates the I-V characteristic curve for the SLARC result with different wavelengths using PC1D simulation. The curve at wavelength 250 nm has the lowest relationship with the current and voltage. The curve at wavelength 600 nm has the highest, which is 23.42%, followed by a wavelength of 700 nm, which is slightly different at 23.27%. The wavelength of incident light is also critical with respect to the interaction of light with the ARC and the solar cell. The ARC manifests in controlling the incident light for specific wavelengths through proper design of the refractive index and thickness of the ARC material, which acts to enhance the efficiency of the solar cell [9]. The application of ARC has improved the I_{sc} from 1.73 A to 2.39 A, which indicating the improvement of light absorption, current generation [14], leading to the increase of device efficiency and photoelectric conversion [8], [11].

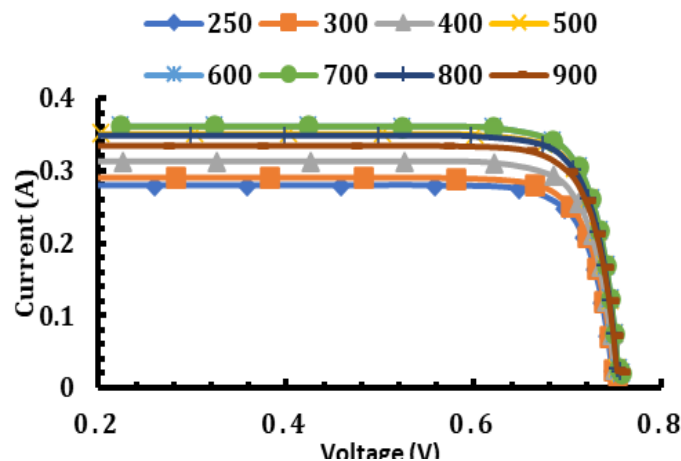


Fig. 4. I-V characteristic curve for SLARC.

Figure 5 shows the characteristic curve of DLARC of ZnO/TiO₂. Wavelength at 500 nm has the highest point in the I-V curve, and the lowest point in the I-V curve is at wavelength 300 nm. The gap between these wavelengths highest point is just slightly different and unnoticeable. The wavelength plays a role in the interaction of the light with the ARC and the solar cell. The refractive index of the selected ARC material, alongside its thickness, may be adjusted to maximise the light

management at specific wavelength regions, resulting in an overall improvement in solar cell performance [9].

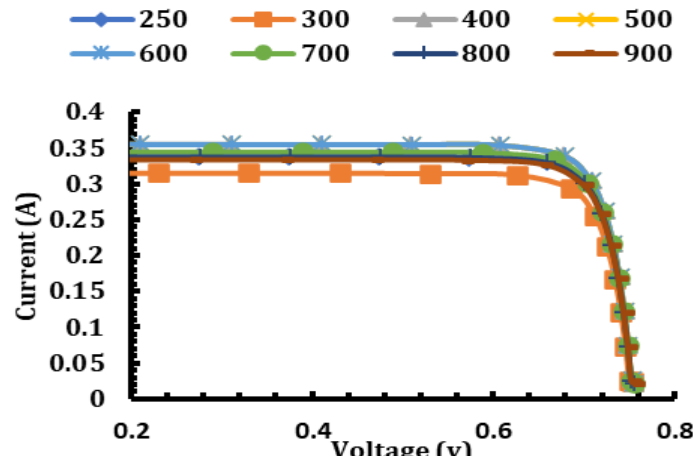


Fig. 5. I-V characteristic curve for DLARC.

Figure 6 shows the I-V characteristics among devices with no ARC, SLARC, and DLARC simulated in PC1D. The highest point is ZnO SLARC, followed by ZnO/TiO₂ DLARC. Lastly, the lowest point is the no ARC curve. The gap between SLARC and DLARC is very little. SLARC is typically less layered, which can simplify fabrication and improve light interaction with the active layer of the solar cell. That can mean fewer interfaces at which light could be lost through reflection or scattering [11]. The result is that SLARC greatly minimises light reflection away from the solar cell and maximises light penetration into the cell for electricity generation by simply tailoring the refractive index of this coating to match that of silicon. In a single-layer ARC, light interacts with a more single interface, reducing the likelihood of destructive force that could arise in multi-layer structures. Such anti-reflective layers can thus increase light transmission into the solar cell and reduce reflectance [11]. DLARCs can expand reflectance suppression across a wider spectral range, but at the cost of increased angular dependence. While DLARCs can reach lower reflectance minimums, they can also have more variability of reflectance under varying angles of incidence that can hurt efficiency during real-world application [16]. There are many concepts of optical phenomena involved in explaining the possible actual process when the sunlight arrives at a solar cell surface. The main characteristics of optical investigation are reflectance, absorption, and transmission. One must realise the better performance of solar cells is the reduction of light reflection and the enhancement of light absorption and transmission of the solar cells. For the extended work, the wafer ray tracer is used to validate the single and double ARC on GaAs-based solar cells. The range of wavelengths used in this work is from 300 nm to 120 nm. The reflection, absorption, and transmission were investigated.

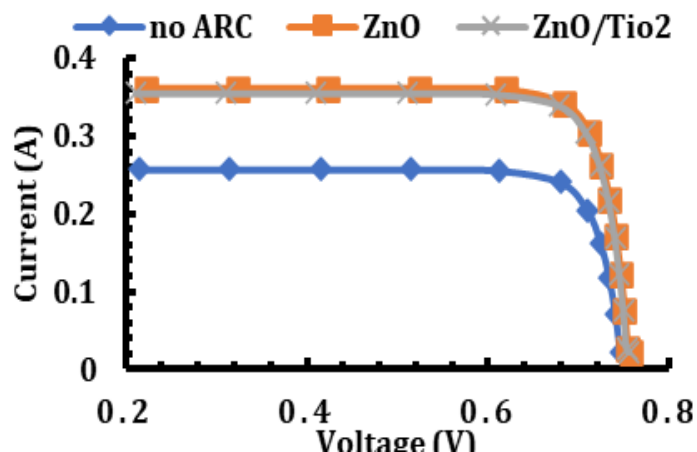


Fig. 6. I-V characteristic curve for no ARC, SLARC, and DLARC.

Figure 7 shows the absorption of double ZnO/TiO₂, DLARC and ZnO SLARC on the GaAs-based solar cells. The absorption without ARC is also included as a comparison. Both DLARC and SLARC presented higher absorption values compared to without ARC. DLARC and SLARC have proven that more photons are absorbed, resulting in a higher current compared to without ARC. The findings are in good agreement with the result from figure 5. Overall, the DLARC shows the lowest reflectivity in the range of 300 to 440 nm but is higher than a single ARC between 440 nm and 800 nm.

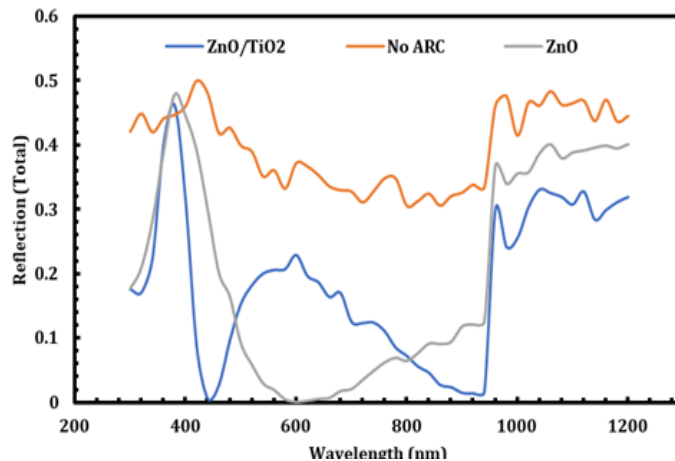


Fig. 7. Reflection curve for GaAs with ZnO/TiO₂, DLARC and ZnO SLARC. Reference without ARC GaAs included as a comparison.

Figure 8 is consistent with Figure 7, showing that reduced reflection allows more photons to be absorbed by the device. An ultra-thin active layer promotes lower recombination currents, higher V_{oc} , and improved device efficiency when light absorption is enhanced [17]. As the absorption rate increases, the photo-generated current also rises, positively impacting the efficiency of the solar cell device [3]. By using an ARC layer, light absorption improves across the entire range of silicon-based solar cells, highlighting the importance of enhanced photon absorption in boosting solar cell efficiency [18]. Generally, traditional ARCs have lower transmission efficiency across the solar spectrum.

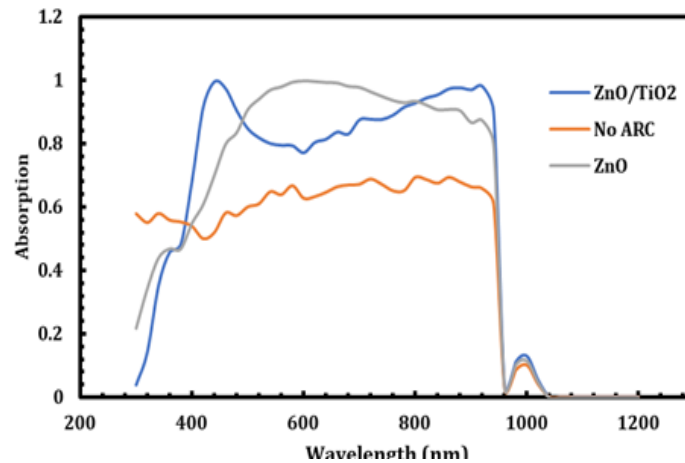


Fig. 8. Absorption curve for GaAs with double ARC, ZnO/TiO₂, and single ARC, ZnO. Reference without ARC GaAs included as a comparison.

Figure 9 shows the transmission graphs of DLARC, SLARC, and without ARC for solar cell devices. Higher transmission responses were detected for DLARC and SLARC compared to without an ARC layer. DLARC shows its suitability to capture more incident light entering the device compared to SLARC. The reduced light reflection and transmission spectra were spotted in the range of 300 and 1200 nm, which is in parallel with Table 3 and Table 4.

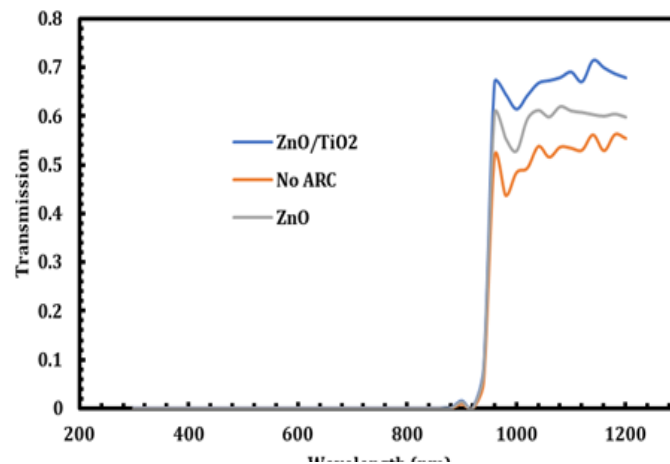


Fig. 9. Transmission curve for GaAs with double ARC, ZnO/TiO₂, and single ARC, ZnO. Reference without ARC GaAs included as a comparison.

4. Conclusion

As a conclusion, we were successfully simulated the various ARCs on the solar cell's devices. We found that the highest efficiency was calculated as 23.42% for ZnO SLARC with a thickness of 78.411 nm, followed by the ZnO/TiO₂ DLARC (63.516 nm/50.403 nm), contributing to 23.04%. Our wafer ray tracer simulator results showed a similar trend with PC1D findings, where higher transmission and lower absorption spectra were observed to device with SLARC and DLARC compared without ARC layer, allowing more incident light to be captured by the device.

Acknowledgments

The support from Universiti Teknologi Mara, Shah Alam is also gratefully acknowledged.

References

- [1] R. Sharma, A. Gupta, A. Viridi, *Journal of Nano- and Electronic Physics* 9(2) (2017).
- [2] Y. F. Makableh, H. Alzubi, G. Tashtoush, *Coatings* 11(6), 721 (2021); <https://doi.org/10.3390/coatings11060721>
- [3] K. Ali, S. A. Khan, M. Z. Mat Jafri, *International Journal of Electrochemical Science* 9(12), 7865 (2014); [https://doi.org/10.1016/S1452-3981\(23\)11011-X](https://doi.org/10.1016/S1452-3981(23)11011-X)
- [4] A. Luque, A. Luque, A. Martí, A. Martí, *Theoretical Limits of Photovoltaic Conversion and New-Generation Solar Cells* (2011); <https://doi.org/10.1002/9780470974704.ch4>
- [5] J. Hossain, *Journal of Physics Communications* 5(8) (2021).
- [6] G. Hashmi, M. J. Rashid, Z. H. Mahmood, M. Hoq, M. H. Rahman, *Journal of Theoretical and Applied Physics* 12(4), 327 (2018); <https://doi.org/10.1007/s40094-018-0313-0>
- [7] M. Beye, M. E. Faye, A. Ndiaye, F. Ndiaye, A. S. Maiga, *Research Journal of Applied Sciences, Engineering and Technology* 6(3), 412 (2013); <https://doi.org/10.19026/rjaset.6.4094>
- [8] D. Parajuli, G. S. Gaudel, D. Kc, K. B. Khattri, W. Y. Rho, *AIP Advances* 13(8) (2023); <https://doi.org/10.1063/5.0153197>
- [9] N. I. I. M. Jamaluddin, M. Z. M. Yusoff, M. F. Malek, *Trends in Sciences* 21(3) (2024); <https://doi.org/10.48048/tis.2024.7337>
- [10] A. Luque, G. Sala, W. Palz, G. Santos, P. Helm, *Tenth E.C. Photovoltaic Solar Energy Conference* (1991); <https://doi.org/10.1007/978-94-011-3622-8>
- [11] G. Hashmi, A. R. Akand, M. Hoq, H. Rahman, *Silicon* 10(4), 1653 (2018); <https://doi.org/10.1007/s12633-017-9649-3>
- [12] D. A. Clugston, P. A. Basore, *PC1D VERSION 5: 32-bit Solar Cell Modeling on Personal Computers* (1997).
- [13] K. A. Salman, *Solar Energy* 147, 228 (2017); <https://doi.org/10.1016/j.solener.2016.12.010>
- [14] W. W. Zhang, H. Qi, Y. K. Ji, M. J. He, Y. T. Ren, Y. Li, *Solar Energy* 230, 1122 (2021); <https://doi.org/10.1016/j.solener.2021.11.031>
- [15] D. Jovanović, R. Gajić, K. Hingerl, *Science of Sintering* 40(2), 167 (2008); <https://doi.org/10.2298/SOS0802167J>
- [16] K. Ali, S. A. Khan, M. Z. Mat Jafri, *Solar Energy* 101, 1 (2014); <https://doi.org/10.1016/j.solener.2013.12.021>
- [17] R. A. Pala, J. White, E. Barnard, J. Liu, M. L. Brongersma, *Advanced Materials* 21(34), 3504 (2009); <https://doi.org/10.1002/adma.200900331>
- [18] X. Sun, X. Xu, G. Song, J. Tu, L. Li, P. Yan, K. Hu, *Optical Materials* 101, 109739 (2020); <https://doi.org/10.1016/j.optmat.2020.109739>